

Muon spin relaxation study of spin-glass freezing in the Heusler compound $\text{Ru}_{1.9}\text{Fe}_{0.1}\text{CrSi}$ Masahiko Hiroi,^{1,*} Toru Hisamatsu,¹ Takao Suzuki,^{2,3} Kazuki Ohishi,^{3,4} Yasuyuki Ishii,^{3,5} and Isao Watanabe³¹*Department of Physics and Astronomy, Graduate School of Science and Engineering, Kagoshima University, Kagoshima 890-0065, Japan*²*Faculty of Engineering, Shibaura Institute of Technology, Saitama 337-8570, Japan*³*Advanced Meson Science Laboratory, RIKEN Nishina Center for Accelerator-Based Science, 2-1 Hirosawa, Wako, Saitama 351-0198, Japan*⁴*CROSS, JAEA, 162-1 Shirakata, Tokai, Naka, Ibaraki 319-1106, Japan*⁵*Department of Physics, Tokyo Medical University, 6-1-1 Shinjuku, Tokyo 160-8402, Japan*

(Received 7 October 2010; revised manuscript received 15 May 2011; published 12 July 2013)

In the temperature dependence of magnetization, the Heusler compound $\text{Ru}_{1.9}\text{Fe}_{0.1}\text{CrSi}$ exhibits a peak at a temperature which is defined as T_N^* . Below that temperature strong irreversibility occurs, the onset temperature of which is defined as T_g . However, no evidence of long-range order has been found. In this study the magnetic properties of these anomalies were investigated using zero-field (ZF) and longitudinal-magnetic-field (LF) muon-spin-relaxation (μSR) measurements. In the temperature dependence of the relaxation rate of ZF- μSR , a peak at ~ 16 K was observed, which agrees with T_g . LF- μSR measurements as a function of magnetic field reveal the existence of a static internal magnetic field at 0.3 K. Around $T_N^* \sim 30$ K, we detected no anomalies that can be associated with a magnetic phase transition in the temperature dependence of the relaxation rate of μSR , but a large decrease in the initial asymmetry was observed. LF- μSR measurements suggest that the internal magnetic field appears even around T_N^* . These results suggest that around T_N^* independent spin-frozen regions form inhomogeneously. With decreasing temperature these regions gradually develop, and eventually, at T_g spin-glass freezing occurs with correlations over the whole sample.

DOI: [10.1103/PhysRevB.88.024409](https://doi.org/10.1103/PhysRevB.88.024409)

PACS number(s): 75.50.Lk, 76.75.+i, 72.80.Ga, 75.30.Kz

I. INTRODUCTION

Heusler compounds have the formula X_2YZ , where X and Y are transition elements and Z is an sp element, and they have a cubic $L2_1$ structure. Recently, these compounds have attracted growing interest because of their potential use as half metals,¹⁻³ ferromagnetic shape memory alloys, and thermoelectric materials. Half metals are ferromagnetic metals with conduction electrons that are 100% spin polarized. Ishida *et al.* predicted that the Heusler compound Co_2MnZ ($Z = \text{Si}$ or Ge) would be a half metal through a first-principles band structure calculation.^{4,5} However, the realization of high spin polarization in Heusler compounds has been difficult because disorder in the crystals is believed to reduce spin polarization. To overcome this difficulty Heusler compounds $\text{Ru}_{2-x}\text{Fe}_x\text{CrSi}$ were theoretically proposed to be complete or nearly complete half metals that are robust to chemical disorders.^{6,7} Motivated by this work, we prepared samples of $\text{Ru}_{2-x}\text{Fe}_x\text{CrSi}$ and found that those for $x \geq 0.5$ were ferromagnetic and that the Curie temperature for $x \gtrsim 1.5$ was much higher than room temperature.^{8,9} These results reveal that the Fe-rich $\text{Ru}_{2-x}\text{Fe}_x\text{CrSi}$ ($x \sim 2$) is a promising candidate as a material that has high spin polarization and is robust to disorder. Recently, we have found from magnetic-susceptibility and specific-heat measurements^{10,11} that Ru_2CrSi exhibits an antiferromagnetic transition at $T_N = 13$ K. For the analogous compound Ru_2CrGe an antiferromagnetic order has already been found,¹²⁻¹⁴ in particular the neutron-diffraction measurements revealed an antiferromagnetic structure in which the magnetic moment is carried by the Cr atoms.¹³ A theoretical calculation also shows the stability of antiferromagnetism in Ru_2CrSi .^{6,15}

Thus, competition between ferromagnetism and antiferromagnetism is expected for Ru-rich $\text{Ru}_{2-x}\text{Fe}_x\text{CrSi}$, although magnetic frustration in Heusler compounds has not received

much attention. In $\text{Ru}_{1.9}\text{Fe}_{0.1}\text{CrSi}$ ferromagnetic order is absent, while a peak in the temperature dependence of magnetization $M(T)$ appears at ~ 30 K, which is defined as T_N^* .⁹ At first, this peak was assumed to indicate an antiferromagnetic transition because a peak in $M(T)$ was observed at T_N in Ru_2CrSi .^{10,11} However, in the electrical resistivity⁹ and the specific heat,^{16,17} anomalies that indicate a phase transition were not found. Meanwhile, at temperatures below T_N^* , a separation was found between $M(T)$ measured in a zero-field-cooling process (ZFC) and in a field-cooling process (FC). This suggests the formation of a spin-glass (SG) state. Furthermore, the separation increased rapidly from a temperature lower than T_N^* .¹⁶ This temperature was regarded as the onset of (strong) irreversibility, which is defined as T_g . We found that T_N^* and T_g had different magnetic field dependences. Although T_g depends on the magnetic field H , T_N^* changes only slightly with H . We estimated T_g at $H = 0$ to be ~ 15 K by extrapolating T_g observed in magnetic fields to $H = 0$. A broad peak in the magnetic specific heat divided by temperature $C_m(T)/T$ occurred around T_g , which suggests a conventional SG transition, whereas T^2 dependence of the specific heat has been observed at temperatures below T_g ;¹⁷ this differs from the linear T dependence observed in conventional SG states. These observations suggest the absence of an antiferromagnetic transition at T_N^* and the appearance of unconventional SG states.

In previous papers,^{16,17} the anomalies at T_g and T_N^* were interpreted as successive SG transitions. Theories of a Heisenberg SG model predict successive SG transitions in the presence of a magnetic field. As temperature decreases from the paramagnetic phase, the freezing of spin components transverse to the magnetic field occurs first; this boundary is called a Gabay-Toulouse (GT) transition.^{18,19} As temperature decreases further, the freezing of components longitudinal

to the field occurs; this is the de Almeida–Thouless (AT) transition.²⁰ The observed magnetic phase diagram of the boundaries T_g and T_N^* for $\text{Ru}_{1.9}\text{Fe}_{0.1}\text{CrSi}$ seems to be qualitatively described by AT and GT transitions. In other materials, observations of similar magnetic phase diagrams^{21,22} and characteristic irreversibilities in $M(T)$,^{23,24} such as found in $\text{Ru}_{1.9}\text{Fe}_{0.1}\text{CrSi}$, have been reported and interpreted in terms of successive SG transitions.

To our knowledge, successive SG transitions have not been confirmed by microscopic probes. Therefore the origins of the magnetic phase diagram and the characteristic irreversibility in $M(T)$ have not been clarified. So far, microscopic information on $\text{Ru}_{1.9}\text{Fe}_{0.1}\text{CrSi}$ is lacking, and thus the origins of the anomalies in $M(T)$ are not fully understood. Therefore we have performed zero-field (ZF) and longitudinal-field (LF) muon-spin-relaxation (μSR) measurements to clarify whether or not the anomalies indicate a phase transition and to reveal the nature of the magnetic states at low temperature.

II. EXPERIMENTS

A polycrystalline ingot of $\text{Ru}_{1.9}\text{Fe}_{0.1}\text{CrSi}$ was prepared by arc melting. The crystal structure was confirmed to be $L2_1$ by x-ray diffraction, and the lattice constant was found to be 0.588 nm. The crystal structure and the crystallographic data are shown in Ref. 16. Measurements of μSR were carried out at the RIKEN-RAL Muon Facility²⁵ using a spin-polarized single-pulse positive surface muon (μ^+) beam with a momentum of 27 MeV/c. A few samples were cut from the ingot and mounted on a high-purity silver plate with Apiezon N grease. In μSR measurements, spin-polarized muons are implanted into samples. The muon spin depolarization due to internal fields at the muon sites is described by the asymmetry $A_0(t)$, defined as follows:

$$A_0(t) = \frac{F(t) - \alpha B(t)}{F(t) + \alpha B(t)}. \quad (1)$$

Here $F(t)$ and $B(t)$ are the total muon events counted by the forward and backward counters at time t , respectively, and α is a calibration factor reflecting relative counting efficiencies between the forward and backward counters. Temperature was controlled using a ^4He and a ^3He Oxford cryostat.

III. RESULTS AND DISCUSSION

Figure 1 shows the ZF- μSR time spectra of $\text{Ru}_{1.9}\text{Fe}_{0.1}\text{CrSi}$ at temperatures between 4.3 and 50 K. The time spectra for $T > 40$ K are well fitted with a single exponential function. At lower temperatures a fast relaxation component appears, and the loss of the initial asymmetry is seen. The spectra below 40 K can be expressed as

$$A_0(t) = A_1 \exp(-\lambda_1 t) + A_2 \exp(-\lambda_2 t). \quad (2)$$

The first and second terms represent the fast and the slow relaxation components, respectively, and λ_1 and λ_2 are the muon-spin-relaxation rates for each component. The initial asymmetry A_0 is $A_0(t)$ at $t = 0$: $A_0 = A_1 + A_2$. In the analysis, A_i and λ_i ($i = 1, 2$) are fitting parameters. The time spectra are well fitted with Eq. (2), as shown in Fig. 1. The temperature dependences of A_0 and A_2 in ZF- μSR

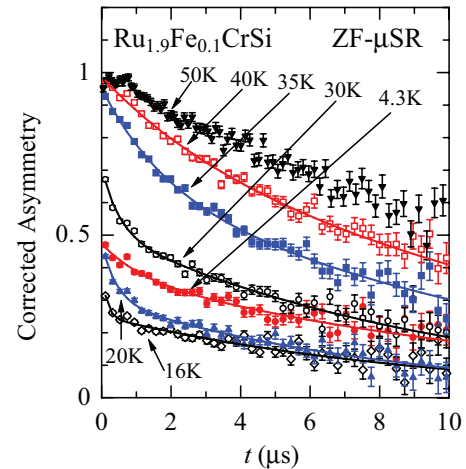


FIG. 1. (Color online) ZF- μSR time spectra of $\text{Ru}_{1.9}\text{Fe}_{0.1}\text{CrSi}$ at various temperatures. Solid lines are fits to Eq. (2).

are shown in Fig. 2(a). With decreasing temperature A_0 decreases and becomes smallest around 12 K. With further decreasing temperature the tails of the spectra shift upward. In general, when a static internal magnetic field develops, 1/3 of the polarization of the muon spins remains owing to the component of the static internal field parallel to the initial muon spin direction; this leads to the slow relaxation tail with the 1/3 value of the asymmetry. Consequently, the observed upward shift can be interpreted as a recovery to the 1/3 tail and suggests the development of a static internal field at low temperatures. This is confirmed by LF- μSR , as explained below. Figure 2(b) shows the temperature dependence of the muon-spin-relaxation rates λ_1 and λ_2 in ZF- μSR in Eq. (2). Both λ_1 and λ_2 show a maximum at ~ 16 K. This suggests that spin freezing occurs at ~ 16 K.

To investigate whether or not a static internal magnetic field develops, LF- μSR measurements were carried out at 0.3 K for different values of the longitudinal magnetic field H_{LF} , up to 3950 Oe. The time spectra of LF- μSR at 0.3 K are shown

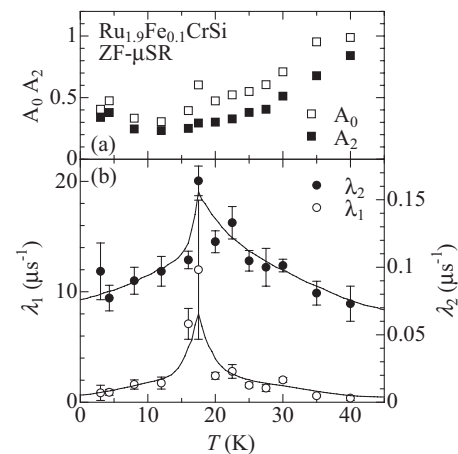


FIG. 2. (a) Temperature dependence of the initial asymmetry $A_0 = A_1 + A_2$ and A_2 in ZF- μSR . (b) Temperature dependence of the relaxation rates λ_1 (left vertical axis, open circles) and λ_2 (right vertical axis, solid circles) in Eq. (2) for ZF- μSR . Solid lines are guides to the eye.

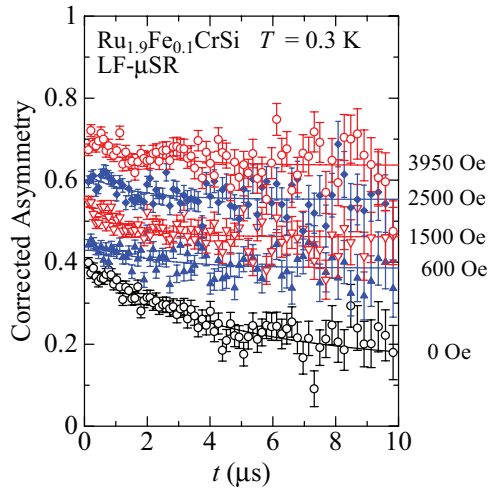


FIG. 3. (Color online) LF- μ SR time spectra for various longitudinal magnetic fields at 0.3 K. Solid lines are fitted results.

in Fig. 3. The time spectra are well fitted with Eq. (2). The long tails of the time spectra following fast relaxation increase with increasing H_{LF} . This is typical behavior in the presence of a static internal magnetic field at the muon sites H_{int} .²⁶ In general, implanted muon spins precess around the total magnetic field of the internal and external fields at the muon sites. The increasing external longitudinal field decouples the muon spins from the internal field, which leads to the upward shift of the long horizontal tails of the time spectra. H_{int} is estimated using the following equation:

$$A_{\infty} = \frac{3}{4} - \frac{1}{4x^2} + \frac{(x^2 - 1)^2}{16x^3} \ln \frac{(x + 1)^2}{(x - 1)^2}, \quad (3)$$

where $x = H_{LF}/H_{int}$ (Refs. 27–30) and A_{∞} is the residual asymmetry left after a long time. We consider the H_{LF} dependence of A_0 to represent A_{∞} in this case, as seen in Fig. 3. The H_{LF} dependence of A_0 at 0.3 K is plotted in Fig. 4. The solid line shown in Fig. 4 is the best fit obtained using Eq. (3) after applying corrections for instrument backgrounds. We evaluated the value of H_{int} to be approximately 1308 ± 50 Oe.

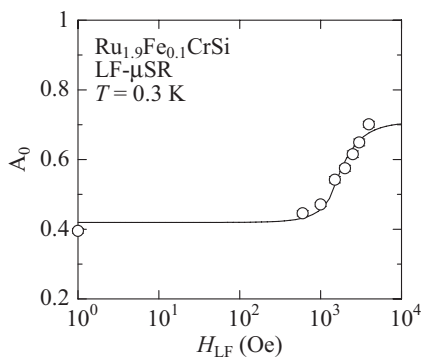


FIG. 4. Dependence of the initial asymmetry A_0 on the longitudinal field H_{LF} at 0.3 K for LF- μ SR. A_0 observed in zero field is plotted at $H_{LF} = 1$ Oe. The best fit obtained using Eq. (3) is shown by the solid line. The static internal field is evaluated to be approximately 1308 ± 50 Oe.

This value is probably an underestimate because the data are limited to $H_{LF} = 3950$ Oe.

The results of LF- μ SR explained above demonstrate the presence of a static internal magnetic field at low temperatures. The maxima in the relaxation rates were observed at ~ 16 K. This suggests that spin freezing or a phase transition occurs at this temperature, which almost coincides with T_g estimated from $M(T)$. However, a discontinuity in specific heat, indicating a phase transition to long-range order, was not found around this temperature or at any other temperature. Instead, a broad peak in $C_m(T)/T$ was found around this temperature.¹⁷ When these results are considered together, we conclude that SG freezing occurs at T_g .

However, although a peak in magnetic susceptibility was found at $T_N^* \sim 30$ K, the result for the specific heat indicates that there is no phase transition to long-range order. As seen in Fig. 2, in the ZF- μ SR results around T_N^* an anomaly indicating a phase transition seems to be absent in the relaxation rates, whereas a large but rather gradual decrease appears in the initial asymmetry. To investigate in more detail whether or not there is a magnetic transition around T_N^* , we performed μ SR measurements between 10 and 60 K in a longitudinal field of 100 Oe; this field was applied to decouple the nuclear spin contribution and to extract the effects of electron spins.

Figure 5 shows the time spectra at $H_{LF} = 100$ Oe for various temperatures. The time spectra are well fitted with Eq. (2). The temperature dependences of the initial asymmetry A_0 and A_2 at $H_{LF} = 100$ Oe are shown in Fig. 6(a). The temperature dependences of λ_1 and λ_2 at $H_{LF} = 100$ Oe are shown in Fig. 6(b). The tendencies in the temperature dependences of λ_1 and λ_2 are similar. Both λ_1 and λ_2 are almost constant above ~ 40 K, and with decreasing temperature from 40 to 20 K, they increase gradually. Freezing is considered to occur at ~ 15 K because T_g at 100 Oe seems to be at most ~ 0.5 K lower than T_g at 0 Oe. We also notice that T_N^* at 100 Oe is practically the same temperature as T_N^* at 0 Oe.¹⁶ In these results, as in ZF- μ SR, we did not find an anomaly in the relaxation rates that could be associated with a magnetic phase transition around T_N^* , whereas a decrease in the initial asymmetry was observed.

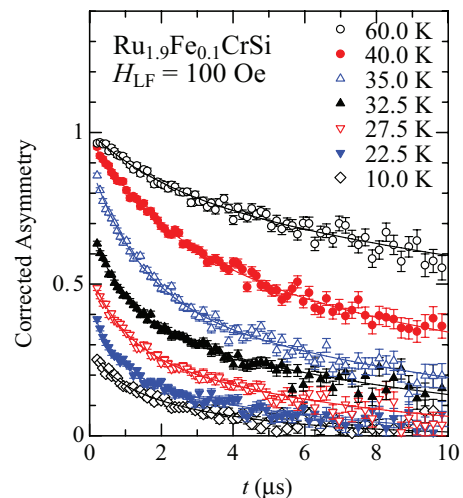


FIG. 5. (Color online) Time spectra of μ SR at $H_{LF} = 100$ Oe at various temperatures. Solid lines are fitted results.

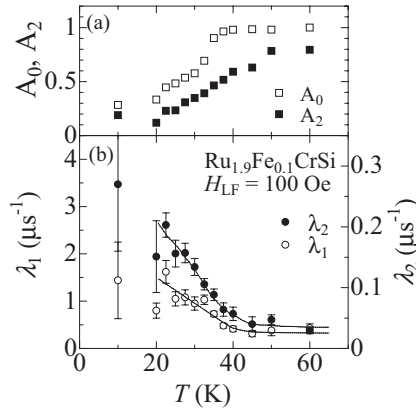


FIG. 6. (a) Temperature dependence of the initial asymmetry $A_0 = A_1 + A_2$ and A_2 at $H_{LF} = 100$ Oe. (b) Temperature dependence of the relaxation rates λ_1 (left vertical axis, open circles) and λ_2 (right vertical axis, solid circles) in Eq. (2) in $H_{LF} = 100$ Oe. Solid lines are guides to the eye.

To investigate the origin of the large decrease in the initial asymmetry below ~ 40 K and the characteristics of the magnetic state between T_g and $\sim T_N^*$, we performed LF- μ SR measurements as a function of magnetic field at temperatures between 8 and 40 K. Representative time spectra at 25 K are shown in Fig. 7. Those spectra are well fitted with Eq. (2), except for those at 40 K, which are well fitted with a single exponential function. The time spectra change with H_{LF} . In the presence of a static field A_2 is expected to change with H_{LF} in the manner of A_∞ in Eq. (3), and thus the H_{LF} dependence of A_2 is analyzed using Eq. (3), as shown in Fig. 8. In Fig. 8 it appears that, at temperatures below 30 K, A_2 increases from approximately the same field as at 0.3 K, as shown in Fig. 4. This analysis suggests that a static field arises at the muon site from temperatures higher than $T_N^* \sim 30$ K, and below ~ 30 K the value of the static field does not change much.

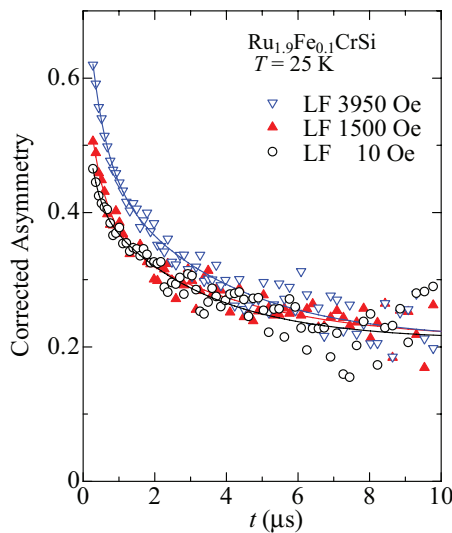


FIG. 7. (Color online) Representative LF- μ SR time spectra at 25 K for longitudinal magnetic fields of 10, 1500, and 3950 Oe. Solid lines are fitted results.

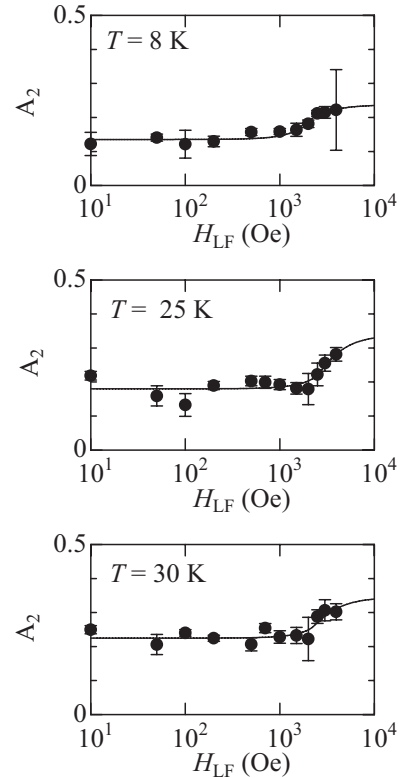


FIG. 8. Dependence of the asymmetry of the slow relaxation component in Eq. (2), A_2 , on the longitudinal field H_{LF} for LF- μ SR at 8, 25, and 30 K. The best fits obtained using Eq. (3) are shown by the solid lines. A static internal field appears to arise even around 30 K.

The relaxation rates of μ SR showed no anomaly that would indicate a phase transition at T_N^* . However, from ~ 40 K, which is higher than T_N^* , we observed an increase in the relaxation rates and a large but gradual decrease in the initial asymmetry for ZF- μ SR and LF- μ SR at $H_{LF} = 100$ Oe. Moreover, the LF- μ SR measurements as a function of magnetic field at temperatures below 40 K suggest that internal fields as large as those at low temperatures arise even from $\sim T_N^*$; these internal fields are independent of temperature. These results indicate an inhomogeneous magnetic state.³¹ From ~ 40 K the formation of independent spin-frozen regions begins. These static regions extend gradually as temperature decreases. This causes the observed decrease in the initial asymmetry because the loss in the initial asymmetry approximately corresponds to the volume fraction of regions with a static field. With decreasing temperature the correlation between static regions becomes larger, and eventually a spin-frozen state with correlations over the whole sample is formed at $\sim T_g$, which we have regarded as SG freezing.

Note that inhomogeneous magnetic states that emerge prior to freezing or a phase transition are sometimes considered. The appearance of inhomogeneous magnetic states prior to ferromagnetism have been discussed in frustrated and disordered materials.³²⁻³⁴ Furthermore, in bilayer manganite without long-range order, an inhomogeneous magnetic state prior to spin freezing was reported in a μ SR measurement.³⁵

Then we consider the relation of the above interpretation to the successive SG transitions. We have concluded that

below $\sim T_N^*$ an inhomogeneous magnetic state is realized. If the spin components transverse to the magnetic field freeze first inhomogeneously, this freezing might be seen as the GT transition. Then if the remaining spin freedom freezes at a still lower temperature, T_g , this process can be regarded as successive SG transitions. The present results seem consistent with this interpretation. However, in our results the change around T_N^* proceeds gradually and appears like a crossover, whereas the freezing at T_g appears more like a transition. This differs from the theoretically proposed AT and GT transitions, in which the GT transition is described as a phase transition and the AT transition as a crossover.

IV. CONCLUSIONS

For $\text{Ru}_{1.9}\text{Fe}_{0.1}\text{CrSi}$ we found a peak-type anomaly at $T_N^* \sim 30$ K and an irreversibility-type anomaly at $T_g \sim 16$ K

in $M(T)$ measurements and the absence of long-range order from specific-heat measurements. In this study we investigated magnetic properties of $\text{Ru}_{1.9}\text{Fe}_{0.1}\text{CrSi}$ by μSR measurements. From the ZF- and LF- μSR studies we obtained clear evidence for spin freezing at T_g . At T_g the onset of a strong irreversibility in $M(T)$ and, in addition, a broad peak in $C_m(T)/T$ were found. From these characteristics we concluded that SG freezing occurs at T_g . Around T_N^* no indication of a phase transition or spin freezing was found, but the appearance of an inhomogeneous magnetic state was suggested.

ACKNOWLEDGMENT

This work was supported by the KEK-MSL Inter-University Program for Overseas Muon Facilities.

*hiro@sci.kagoshima-u.ac.jp

¹I. Galanakis, P. H. Dederichs, and N. Papanikolaou, *Phys. Rev. B* **66**, 174429 (2002).

²M. I. Katsnelson, V. Y. Irkhin, L. Chioncel, A. I. Lichtenstein, and R. A. de Groot, *Rev. Mod. Phys.* **80**, 315 (2008).

³C. Felser, G. Fecher, and B. Balke, *Angew. Chem. Int. Ed.* **46**, 668 (2007).

⁴S. Ishida, S. Fujii, S. Kashiwagi, and S. Asano, *J. Phys. Soc. Jpn.* **64**, 2152 (1995).

⁵S. Ishida, T. Masaki, S. Fujii, and S. Asano, *Phys. B* **245**, 1 (1998).

⁶S. Mizutani, S. Ishida, S. Fujii, and S. Asano, *Mater. Trans.* **47**, 25 (2006).

⁷S. Ishida, S. Mizutani, S. Fujii, and S. Asano, *Mater. Trans.* **47**, 31 (2006).

⁸K. Matsuda, M. Hiroi, and M. Kawakami, *J. Phys. Condens. Matter* **17**, 5889 (2005); **18**, 1837(E) (2006).

⁹M. Hiroi, K. Matsuda, and T. Rokkaku, *Phys. Rev. B* **76**, 132401 (2007).

¹⁰M. Hiroi, H. Ko, S. Nakashima, I. Shigeta, M. Ito, H. Manaka, and N. Terada, *J. Phys. Conf. Ser.* **400**, 032020 (2012).

¹¹M. Hiroi, K. Uchida, I. Shigeta, M. Ito, K. Koyama, S. Kimura, and K. Watanabe, *J. Korean Phys. Soc.* **62**, 2068 (2013).

¹²H. Okada, K. Koyama, K. Watanabe, Y. Kusakari, T. Kanomata, and H. Nishihara, *Appl. Phys. Lett.* **92**, 062502 (2008).

¹³P. J. Brown, A. P. Gandy, T. Kanomata, Y. Kusakari, A. Sheikh, K.-U. Neumann, B. Ouladdiaf, and K. R. A. Ziebeck, *J. Phys. Condens. Matter* **20**, 455201 (2008).

¹⁴H. Okada, Y. Kusakari, E. Matsuoka, H. Onodera, K. Koyama, K. Watanabe, and T. Kanomata, *J. Phys. Conf. Ser.* **150**, 042153 (2009).

¹⁵M. Hiroi, T. Rokkaku, S. Mizutani, S. Fujii, and S. Ishida, *J. Phys. Conf. Ser.* **150**, 042058 (2009).

¹⁶M. Hiroi, T. Rokkaku, K. Matsuda, T. Hisamatsu, I. Shigeta, M. Ito, T. Sakon, K. Koyama, K. Watanabe, S. Nakamura, T. Nojima, T. Nakano, L. Chen, T. Fujiwara, Y. Uwatoko, H. Manaka, and N. Terada, *Phys. Rev. B* **79**, 224423 (2009).

¹⁷M. Ito, T. Hisamatsu, T. Rokkaku, I. Shigeta, H. Manaka, N. Terada, and M. Hiroi, *Phys. Rev. B* **82**, 024406 (2010).

¹⁸M. Gabay and G. Toulouse, *Phys. Rev. Lett.* **47**, 201 (1981).

¹⁹D. M. Cragg, D. Sherrington, and M. Gabay, *Phys. Rev. Lett.* **49**, 158 (1982).

²⁰J. R. L. de Almeida and D. J. Thouless, *J. Phys. A* **11**, 983 (1978).

²¹G. G. Kenning, D. Chu, and R. Orbach, *Phys. Rev. Lett.* **66**, 2923 (1991).

²²K. Miyoshi, Y. Nishimura, K. Honda, K. Fujiwara, and J. Takeuchi, *J. Phys. Soc. Jpn.* **69**, 3517 (2000).

²³P. Amornpitoksuk, D. Ravot, A. Mauger, and J. C. Tedenac, *Phys. Rev. B* **77**, 144405 (2008).

²⁴F. Kariya, S. Ebisu, and S. Nagata, *J. Solid State Chem.* **182**, 608 (2009).

²⁵T. Matsuzaki, K. Ishida, K. Nagamine, I. Watanabe, G. H. Eaton, and W. G. Williams, *Nucl. Instrum. Methods Phys. Res., Sect. A* **465**, 365 (2001).

²⁶Y. J. Uemura, T. Yamazaki, D. R. Harshman, M. Senba, and E. J. Ansaldo, *Phys. Rev. B* **31**, 546 (1985).

²⁷I. Watanabe, M. Akoshima, Y. Koike, S. Ohira, and K. Nagamine, *Phys. Rev. B* **62**, 14524 (2000).

²⁸K. Hachitani, H. Fukazawa, Y. Kohori, I. Watanabe, C. Sekine, and I. Shirovani, *Phys. Rev. B* **73**, 052408 (2006).

²⁹F. L. Pratt, *J. Phys. Condens. Matter* **19**, 456207 (2007).

³⁰T. Suzuki, I. Watanabe, F. Yamada, Y. Ishii, K. Ohishi, Risdiana, T. Goto, and H. Tanaka, *Phys. Rev. B* **80**, 064407 (2009).

³¹I. Watanabe, N. Oki, T. Adachi, H. Mikuni, Y. Koike, F. L. Pratt, and K. Nagamine, *Phys. Rev. B* **73**, 134506 (2006).

³²C. He, M. A. Torija, J. Wu, J. W. Lynn, H. Zheng, J. F. Mitchell, and C. Leighton, *Phys. Rev. B* **76**, 014401 (2007).

³³Y. Shimada, S. Miyasaka, R. Kumai, and Y. Tokura, *Phys. Rev. B* **73**, 134424 (2006).

³⁴S. Guo, D. P. Young, R. T. Macaluso, D. A. Browne, N. L. Henderson, J. Y. Chan, L. L. Henry, and J. F. DiTusa, *Phys. Rev. Lett.* **100**, 017209 (2008).

³⁵A. I. Coldea, S. J. Blundell, C. A. Steer, J. F. Mitchell, and F. L. Pratt, *Phys. Rev. Lett.* **89**, 277601 (2002).